Quasilongitudinal soliton in a two-dimensional strongly coupled complex dusty plasma in the presence of an external magnetic field

Samiran Ghosh*
Department of Applied Mathematics, University of Calcutta, 92, Acharya Prafulla Chandra Road, Kolkata-700 009, India
(Received 24 March 2014; revised manuscript received 4 July 2014; published 15 September 2014)

The propagation of a nonlinear low-frequency mode in two-dimensional (2D) monolayer hexagonal dusty plasma crystal in presence of external magnetic field and dust-neutral collision is investigated. The standard perturbative approach leads to a 2D Korteweg-de Vries (KdV) soliton for the well-known dust-lattice mode. However, the Coriolis force due to crystal rotation and Lorentz force due to magnetic field on dust particles introduce a linear forcing term, whereas dust-neutral drag introduce the usual damping term in the 2D KdV equation. This new nonlinear equation is solved both analytically and numerically to show the competition between the linear forcing and damping in the formation of quasilongitudinal soliton in a 2D strongly coupled complex (dusty) plasma. Numerical simulation on the basis of the typical experimental plasma parameters and the analytical solution reveal that the neutral drag force is responsible for the usual exponential decay of the soliton, whereas Coriolis and/or Lorentz force is responsible for the algebraic decay as well as the oscillating tail formation of the soliton. The results are discussed in the context of the plasma crystal experiment.

DOI: 10.1103/PhysRevE.90.033108 PACS number(s): 52.27.Lw, 05.45.Yv

I. INTRODUCTION

The Coulomb complex (dusty) plasma is a many-particle-interacting system consisting of a finite number of charged dust particles. These charged particles interact with each other through a screened strong Coulomb potential and confined by the (electrostatic) external forces [1–3]. In thermodynamic equilibrium, this complex plasma is characterized by two physical parameters: Coulomb coupling constant $\Gamma = Q^2/(4\pi\epsilon_0\Delta T_d)$ (the ratio of the electrostatic potential energy to the thermal energy between two neighboring dust particles) and the screening strength $\kappa = \Delta/\lambda_D$, where ϵ_0 is the permittivity of free space, Q is the dust charge, $\Delta = (3/4\pi n_d)^{1/3}$ represents the mean interdust distance, T_d is the dust kinetic temperature (in units of energy), and λ_D is the plasma Debye length. These two parameters define the screened Coulomb coupling parameter $\Gamma^* = \Gamma\exp(-\kappa)$ to characterize the Coulomb complex (dusty) plasma. The system is called weakly coupled when $\Gamma^* \ll 1$, whereas the system is called strongly coupled when $\Gamma^* > 1$. The dust particles are suspended in a highly ordered state and form crystalline structures when $\Gamma^* \geqslant \Gamma^*_{\rm cr}$ (critical value) $\gg 1$, which is known as dusty plasma crystal [4–6]. Presently, strongly coupled complex plasma (SCCP) is also being considered as the plasma state of soft condensed matter [7]. However, the dusty plasma crystal supports wave modes such as longitudinal and transverse dust-lattice wave (DLW) [8–12].

These DLWs are the reminiscent of wave propagation in atomic chains, which are dominated by nonlinear phenomena, due to intrinsic nonlinearities of interatomic interactions. In absence of an external magnetic field, the dynamics of the linear collective modes and also nonlinear structures such as Mach cones [13–16], solitons [17–26], and also shock [27–29] were extensively studied experimentally and theoretically in two-dimensional (2D) SCCP.

The presence of external magnetic field plays an important and interesting role in SCCP. The presence of an external magnetic field introduces new modes of particle oscillations in a one-dimensional (1D) particle chain in crystals [30]. Later, theoretical investigations [31,32] and molecular dynamics (MD) simulation [31] predict the existence of "upper-hybrid dust-lattice wave," "lower-hybrid dust-lattice wave," and the coupling of these two modes in the presence of a constant external magnetic field in a 2D hexagonal dusty plasma crystal due to the Lorentz force acting on the dust particles. In the presence of a weak magnetic field, the electrons are magnetized, while ions are not magnetized. In the range of strong magnetic field, both electrons and ions are magnetized while the dust particles are still not magnetized. To magnetize the dust particles, an ultrastrong magnetic field is needed because of its extremely low charge-to-mass ratio. Recent experimental observation [33] reveals that for strong magnetic field (in the experiment $B > 2$ T), the plasma system becomes unstable and forms complex patterns due to filamentation of plasma particles. Thus, magnetizing the dust cloud without destroying the background plasma homogeneity for the observation of the propagating waves is extremely challenging [34]. Recently, an alternative approach was proposed [35,36] to magnetize the dust particles (by putting them into a rotating neutral gas column) in a SCCP. On the basis of the well-known Larmor theorem, it is suggested [35,36] that the rotation-induced Coriolis force acts exactly as the Lorentz force in a magnetic field.

It is observed in various experiments [37–44] that the dusty plasma crystal undergoes a complicated rotational dynamic in the presence of an external field. Generally, it is believed that Lorentz force induced $\mathbf{E}\times\mathbf{B}$ (where $\mathbf{E}$ is the radial electric field and $\mathbf{B}$ is the axial magnetic field) ion drift flow is the driving force for the observed dusty plasma crystal rotation and also responsible for the self-rotation of the dust particles. Even, in the absence of external magnetic field, the dust-charging process (the ion flux around the dust-particle surface) is found to be responsible for the spinning motion of the asymmetric dust particle [45,46]. The presence of external magnetic field causes the spinning dust particles to precess

*sran_g@yahoo.com

around the magnetic field direction and significantly modifies the dust particles charging properties [45].

Thus, in presence of external magnetic field, the dust particles experience the Lorentz force and Coriolis force (due to the rotation of dusty plasma crystal). Dust particles also suffers neutral drag force due to the dust-neutral collision in SCCP. In the present work, we want to investigate the effects of these forces on dust particles on the formation of quasilongitudinal localized structures (solitons) of the weakly nonlinear DLW in a 2D SCCP ($\Gamma^* \geqslant \Gamma^*_{\rm cr}$). The well-known reductive perturbation technique (RPT) is used to study the nonlinear dynamics of low-frequency quasilongitudinal DLW. It is found that in presence of Coriolis force and/or Lorentz force on the dust particles and dust-neutral drag force, the dynamics of the nonlinear wave is governed by a new nonlinear equation, which is the combination of the 2D Korteweg-de Vries (KdV) equation, linear forcing, and damping terms. This novel equation is solved analytically and numerically.

The manuscript is organized in the following manner. The effects of external magnetic field on the dust-particle-charging characteristics are discussed in Sec. II. This section also contains the physical assumptions of the problem and the derivation of the nonlinear evolution equation that governs the dynamics of the weakly nonlinear quasilongitudinal DLW. The analytical solution of the nonlinear equation is derived in Sec. III. The numerical simulation of the derived nonlinear equation with the graphical representations are discussed in Sec. IV. Finally, a brief summary of the results and its possible applications are discussed in Sec. V.

II. THEORETICAL MODEL AND QUASILONGITUDINAL NONLINEAR DUST LATTICE WAVE

The strongly coupled complex (dusty) plasma consists of electrons, ions, and the dust particles. The mass of the dust particle is m_d, and the particle gains large negative charge Q. Both Q and m_d are assumed to be constant. The repulsive interdust potential is shielded by the electron-ion plasma, characterized by the constant Debye length λ_D. We consider a monolayer 2D hexagonal lattice as shown Fig. 1. In equilibrium, the particle coordinate is $[x_s = \Delta(n + m/2), y_s = m\sqrt{3}\Delta/2]$, where Δ is the lattice spacing (interdust distance) and $s = (n,m)$ denotes a pair of integers such that $s = \{(0,\pm1),(\pm1,0),(1,-1),(-1,1)\}$. The external static magnetic field $\vec{B}(=B_0\hat{z})$ of field strength B_0 is in the direction perpendicular to the particle layer.

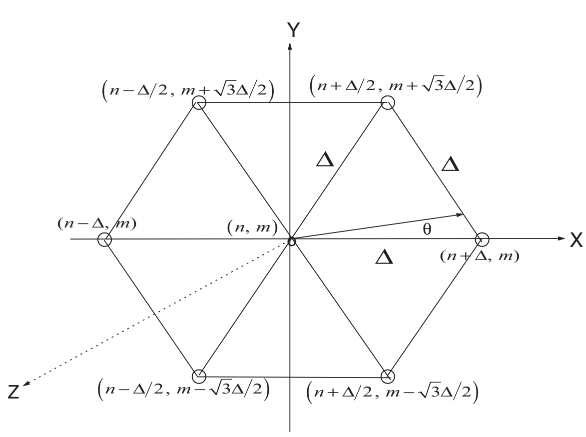

FIG. 1. Elementary single-layer hexagonal 2D crystal centered at (n,m) with lattice spacing Δ. The quasilongitudinal wave propagation vector makes an angle θ with the x axis.

A. Effects of external magnetic field on dust-charging characteristics

Dust particles immersed in plasmas acquire charges by collecting the surrounding ions and electrons. The dust charging can be described by the often used orbit-motion-limited (OML) theory [47,48]. However, the presence of an external magnetic field changes the plasma currents on the dust surface and the magnitude of the dust charge [37,39,45,46,49,50]. To discuss the effects of magnetic field on the equilibrium dust-charging process, we define dimensionless parameter

$$\beta_{B_e} = \frac{a}{\rho_e} = \frac{a}{\rho_i}\sqrt{\frac{\sigma m_i}{m_e}} = \mu\, \beta_{B_i},$$

where $\mu = (\sigma m_i/m_e)^{1/2}, \sigma = T_i/T_e, T_{e(i)}$ is the electron (ion) temperature, $m_{e(i)}$ is the electron (ion) mass, $\rho_{e(i)}$ is the electron (ion) gyroradius, and a is the dust-grain radius. Note that besides the magnetic field, the parameter μ (i.e., temperature and mass ratios) also plays an important role in the dust-charging process. The gyrofrequency of a particle of mass $m_{e(i)}$ and charge (magnitude) e, is given by $\omega_{ce(i)} = eB_0/m_{e(i)}$, while the gyroradius is given by $\rho_{e(i)} = v_\perp/\omega_{ce(i)}$, where $v_\perp$ is the perpendicular velocity component of a charged particle gyrating in a magnetic field. Thus, $\rho_{e(i)}$ is inversely proportional to the magnetic flux density.

In the presence of weak magnetic field when $\beta_{B_e} < 1$, the charging characteristics are not significantly influenced by the existence of external magnetic field, since the curvature effect of the trajectory of an electron (ion) impinging on a dust particle are negligible and in this case the actual charge $Q(= -Ze$, where Z is the number of electrons that reside on the dust particles) of the dust particle is determined by the following relation for $\sigma \ll 1$ [45],

$$\exp(-z) = z/\mu,$$

where $z = Ze^2/4\pi\epsilon_0 aT_e$ is a dimensionless dusty plasma parameter (the ratio of the electrostatic energy of a dust particle of radius a to the electron thermal energy T_e).

As soon as the magnetic field becomes larger than the critical field determined by $\beta_{B_e} \geqslant 1(\beta_{B_i} > 1)$, the electron starts to be magnetized and the electron gyroradius ρ_e becomes small, causing the restriction of electron motion to decrease the probability of electron deposition on the dust particles. Only high-energy magnetized electrons would be involved in the charging process and a fraction of low-energy magnetized electrons would be reflected backwards along the magnetic field direction. As a consequence, the charging cross-section for electrons would be smaller than that in the absence of the magnetic field. The ions will attach to the dust particles with the same rate (as in absence of magnetic field) as the ions are not magnetized and their effective charging cross-section will be much larger than the geometrical cross-section πa^2. The net result is the reduction of dust charge and the effective dust charge $Q_{\rm eff}(=-Z_{\rm eff}e)$ is determined by the relation [45]

$$\exp(-z_{\rm eff})=4z_{\rm eff}/\mu,$$

where $z_{\rm eff}=Z_{\rm eff}e^2/4\pi\epsilon_0 aT_e$ and $Z_{\rm eff}$ is the effective charge number (which is smaller than the actual dust-particle charge number Z). In this case the Lorentz force induced $\mathbf{E}\times\mathbf{B}$ electron drift effect in the vicinity of dust particles is negligible.

However, in presence of a sufficiently strong magnetic field ($\beta_{B_i}\geqslant 1$), the ion starts to be magnetized. Note that this condition can be achieved in experiments for large dust particles and light ions. Actually, for such strong magnetic field, both the ions and electrons in the charging process are magnetized. In this case, the Lorentz force-induced $\mathbf{E}\times\mathbf{B}$ ion drift flow plays an important role and due to this ion flow, the ion shielding close to the dust grain is weak, which results in the increase of the charge number on the dust particles [45,50]. The possible explanation could be the ion acceleration in presence of ion flow. According to the OML theory, this leads to the smaller ion charging cross-section (than that in the absence of a magnetic field) and thus to the smaller ion current to the dust particles, resulting in a more negative charge. The effective dust charge $Q_{\rm eff}$ is determined by the relation [45]

$$\exp(-z_{\rm eff})=\sigma/\mu.$$

The numerical solution [45] shows that in this case for $\mu=100$, $Z_{\rm eff}$ is larger (up to 12 times) than the actual dust-particle charge number Z.

B. Physical assumptions

To formulate the problem, we make the following physical assumptions:

(i) In the presence of strong external magnetic field, the ion flow dynamics is affected and subsequently the dielectric response function [51–53] of the plasma medium. In the presence of a low-frequency ($\omega\ll k_\perp V_{Te}$, $k_\perp$ is the longitudinal wave number, the wave number perpendicular to the direction of magnetic field, and V_{Te} is the electron thermal velocity), long wavelength ($k_\perp\rho_e\ll 1$), and longitudinal oscillation the electron polarization effect is insignificant and the electrons rapidly thermalize along the Z axis to establish a Boltzmann response. Actually, the effect of the magnetic field enters through the modification of the ion susceptibility, which affects the Debye-Hückel (DH) interaction potential (Yukawa potential) and the oscillatory wake-field potential around charged dust grains. Therefore, we consider the modified DH interaction potential [52] between dust particles. In the limit of low-frequency ($\omega\ll\omega_{ci}$) oscillations, the corresponding interdust force between sth and $\acute{s}$th particle becomes

$$\vec{F}_{\acute{s},s}=-\nabla_{\bar{r}_s}\left[\frac{\bar{Q}_{\rm eff}^2}{4\pi\epsilon_0\bar{r}_{\acute{s},s}}\exp\left(-\frac{\bar{r}_{\acute{s},s}}{\lambda_D}\right)\right], \tag{1}$$

where $\bar{Q}_{\rm eff}=Q_{\rm eff}/f^{3/4}$, $\bar{r}_{\acute{s},s}=r_{\acute{s},s}/\sqrt{f}$, $r_{\acute{s},s}=|\vec{r}_{\acute{s},s}|=|\vec{r}_{\acute{s}}-\vec{r}_s|$, $f=(\omega_{pi}/\omega_{ci})^2$, $\omega_{pi}=(n_{i0}e^2/\epsilon_0 m_i)^{1/2}$ is the ion plasma frequency, and $\omega_{ci}(=eB_0/m_i)$ is the ion cyclotron frequency.

(ii) The spinning motion of the asymmetric paramagnetic dust particles resulting in the formation of the magnetic dipole moment [43,45,54,55]. These charged and magnetized dust particles interact with each other due to induced magnetic dipoles via a dipole magnetic force [45,54,55]. However, for small dust particles ($a\leqslant 100\ \mu$m) the interaction due to magnetic force is always weaker than the Coulomb interactions in existing experimental conditions [45] in the crystal formation. Therefore, as a first approximation, we neglect the dust-dust interactions due to magnetic force.

(iii) As mentioned before that the SCCP is characterized by the two parameters: Γ (Coupling parameter) and κ (screening parameter). Presence of external magnetic field modify the DH potential around a stationary dust particle and also the screening parameter. Thus, we define the modified coupling parameter ($\bar{\Gamma}$) and screening parameter ($\bar{\kappa}$) by

$$\bar{\Gamma}=\frac{\Gamma}{f}=\frac{Q_{\rm eff}^2}{4\pi\epsilon_0\Delta f T_d}\quad\text{and}\quad\bar{\kappa}=\frac{\kappa}{\sqrt{f}}=\frac{\Delta}{\sqrt{f}\lambda_D}.$$

This shows that an increase in the external magnetic field results in the increase of the modified coupling parameter and the screening parameter. The screened coupling parameter then becomes $\bar{\Gamma}^*=\bar{\Gamma}\exp(-\bar{\kappa})$. Due to the exponential dependence of $(-\bar{\kappa})$, the strength of the screened coupling parameter reduces with an increase in external magnetic field and therefore higher value of Γ is required for the crystaline state. The Mach cone experiments [13,15,16] (in absence of magnetic field) in 2D monolayer hexagonal dusty plasma crystals reveal that the nearest-neighbor approximation for the interaction is justified for large values of the screening parameter (lattice parameter) κ (in Refs. [13,15], $\kappa\geqslant 1.5$). Therefore, as in the unmagnetized case, we consider $\bar{\kappa}=1.5$ so that dust particles in the monolayer 2D hexagonal crystal (Fig. 1) interact with their six nearest neighbors.

(iv) In the presence of an external magnetic field, the dust particle experiences the Lorentz force $\mathbf{F}_L=m_d\omega_{cd}(\mathbf{v}\times\hat{z})$, where $\mathbf{v}$ is the dust-fluid velocity vector, $\omega_{cd}(=Q_{\rm eff}B_0/m_d)$ is the dust-cyclotron frequency. Dust particles also rotate due to dusty plasma crystal rotation and experience Coriolis force $\mathbf{F}_C=2m_d\omega(\mathbf{v}\times\hat{z})$, where ω is the rotating frequency. The ratio of these two forces becomes

$$\left|\frac{\mathbf{F}_L}{\mathbf{F}_C}\right|=\frac{1}{2}\frac{\omega_{cd}}{\omega}=\frac{1}{2}\left(\frac{Q_{\rm eff}}{m_d}\right)\frac{B_0}{\omega}.$$

This yields that

$$|\,\mathbf{F}_L\,|>|\,\mathbf{F}_C\,|\quad\text{if}\ B_0>\frac{2m_d\omega}{Q_{\rm eff}}.$$

In the experiments in Refs. [37,39,43,45], the observed frequency of rotation $\omega\sim(10-30)$ Hz for $a=5\ \mu$m. This value estimates that Lorentz force dominates over Coriolis force only if $B_0>10^3$ T (because of the small value of the charge-to-mass ratio of dust particles), which is far beyond the present experimental capabilities (implying the dominance of Coriolis force over Lorentz force). Thus, the total force becomes

$$\mathbf{F}=\Omega_r\,(\mathbf{v}\times\hat{z})\,,\quad\text{where}\quad\Omega_r=(2\omega+\omega_{cd})\simeq 2\omega.$$

To include the influence of rotation on quasilongitudinal nonlinear DLW, we assume that Ω_r is low compare to the dust-lattice oscillation frequency $\omega_L \sim O(10^2 - 10^3)$ s^{-1}.

(v) The dust particles collide with the neutral (gas) with frequency $\nu_{\rm dn}$, and therefore they are subject to a weak neutral drag force. In typical plasma crystal experiment [13,19], $\nu_{\rm dn} = (2.4 - 10)$ s^{-1}. Therefore, to include this effect in the nonlinear oscillations, we assume that $\nu_{\rm dn}$ is low compare to ω_L.

(vi) Finally, an external force $F_{\rm ext}$ is often introduced for the initial laser excitation and/or the parabolic confinement to ensure the horizontal lattice equilibrium in experiments [13,21,27]. However, this force $F_{\rm ext}$ has no direct consequence in the formation of soliton in strongly coupled complex plasma [19,20]. Also in the rotating frame, the centrifugal component of the inertial force only softens the horizontal confinement [35]. Therefore, for simplicity, we neglect these forces in the equation of motion.

Next on the basis of these physical assumptions, we consider the equation of motion and the nonlinear dynamics of the quasilongitudinal DLW.

C. Dynamics of quasilongitudinal nonlinear dust-lattice wave

To write the equation of motion due to the action of weak external force, we assume that $\vec{r}_{\acute{s},s} = \vec{r}_{\acute{s},s}(0) + \vec{D}(\acute{s},s)$, where $\vec{r}_{\acute{s},s}(0)$ is the relative equilibrium position and $\vec{D}(\acute{s},s) = d_l(\acute{s},s)\hat{x} + d_t(\acute{s},s)\hat{y}$ is the relative displacement vector of the sth lattice due to the external force, $d_l(\acute{s},s)[= d_l(\acute{s}) - d_l(s)]$ and $d_t(\acute{s},s)[= d_t(\acute{s}) - d_t(s)]$ are, respectively, the $\hat{x}$-direction (longitudinal) and $\hat{y}$-direction (transverse) displacement components. Thus, the equations of motion of the sth particle in the $\hat{x}$ direction and $\hat{y}$ direction are as follows:

$$\begin{aligned}
\frac{\partial^2 d_l}{\partial t^2} &= \frac{\left(\sum_{s\neq\acute{s}} F_{s,\acute{s}}\right)_x}{m_d} + \Omega_r \frac{\partial d_t}{\partial t} - \nu_{\rm dn}\frac{\partial d_l}{\partial t},\\
\frac{\partial^2 d_t}{\partial t^2} &= \frac{\left(\sum_{s\neq\acute{s}} F_{s,\acute{s}}\right)_y}{m_d} - \Omega_r \frac{\partial d_l}{\partial t} - \nu_{\rm dn}\frac{\partial d_t}{\partial t},
\end{aligned} \tag{2}$$

where $d_l \equiv d_l(\acute{s},s)$, $d_t \equiv d_t(\acute{s},s)$, and $s,\acute{s} \in \{(0,\pm1),(\pm1,0),(1,-1),(-1,1)\}$. In the right-hand side of both Eqs. (2), the first term is the X and Y components of the Yukawa force, the second term arises due to the rotation (Coriolis force and/or Lorentz force), and the third term is the neutral drag force.

To study the nonlinear dynamics of the low-frequency small amplitude quasilongitudinal DLW, we adopt the RPT and introduce the following stretched coordinates:

$$\xi = \epsilon\Delta^{-1}(x - \Lambda t), \quad \eta = \epsilon^2\Delta^{-1}y \quad \text{and} \quad \tau = \epsilon^3\omega_L t, \tag{3}$$

where ϵ is a small parameter that measures the strength of the nonlinearity and Λ is the wave velocity. For a quasilongitudinal wave, the transverse displacement (d_t) has a higher-order smallness than that of the longitudinal displacement (d_l) and, therefore, we expand the dependent variables (d_l,d_t) in a power series of ϵ in the following way:

$$d_l = \epsilon d_l^{(1)} + \epsilon^2 d_l^{(2)} + \cdots; \quad d_t = \epsilon^2 d_t^{(1)} + \epsilon^3 d_t^{(2)} + \cdots \tag{4}$$

Also, for the low (compare to ω_L) gyration rate and collisional rate, we consider the following scaling, which are consistent with the perturbation Eqs. (3) and (4):

$$\frac{\Omega_r}{\omega_L} = \Omega\epsilon^2 \quad \text{and} \quad \frac{\nu_{\rm dn}}{\omega_L} = \nu_n\epsilon^3, \tag{5}$$

where both $\Omega \sim O(1)$, $\nu_n \sim O(1)$, i.e., of the order of unity. Note that if Ω_r/ω_L and $\nu_{\rm dn}/\omega_L$ are not so small, one can still use the same substitution but now both Ω and ν_n should be large. This does not present any hurdle to the subsequent theoretical analysis [56].

Next, we assume that the typical scale length of the wave form (characteristic scale length L) is much larger than the lattice spacing Δ, so that $s = (n,m)$ can be considered as a quasicontinuous variable (coordinate). Applying the nearest-neighbor approximation, we expand $D(\acute{s},s)$ in Taylor's series and retain the terms $O(\Delta/L)^4$ [20,22]. Then, substituting Eqs. (3)–(5) in Eq. (2), we obtain the following relations in the lowest order of ϵ:

$$\Lambda = \frac{3}{2\sqrt{2}}C_{\rm DL}; \quad \frac{\partial^2 d_t^{(1)}}{\partial\xi^2} = \frac{\partial^2 d_l^{(1)}}{\partial\xi\partial\eta} + \sqrt{2}\Omega\frac{\partial d_l^{(1)}}{\partial\xi}. \tag{6}$$

Finally, the usual perturbation analysis yields [keeping the terms $O(\epsilon^5)$] the following 2D KdV equation with a linear forcing term due to the rotation of dust particles and a linear damping under the action of mainly Coriolis and neutral drag forces, respectively,

$$\frac{\partial}{\partial\xi}\left[\frac{\partial u}{\partial\tau} - \alpha u\frac{\partial u}{\partial\xi} + \beta\frac{\partial^3 u}{\partial\xi^3} + \nu u\right] + \gamma\frac{\partial^2 u}{\partial\eta^2} = \frac{\Omega^2 u}{\sqrt{2}}, \tag{7}$$

where $u = \Delta^{-1}\partial_\xi d_l^{(1)}$ and

$$\alpha = \frac{3}{16\sqrt{2}}\left[\frac{2\bar{\kappa}^3 + 5\bar{\kappa}^2 + 10\bar{\kappa} + 10}{\bar{\kappa}^2 + 2\bar{\kappa} + 2}\right], \tag{8}$$

and

$$\beta = \frac{11}{192\sqrt{2}}, \quad \nu = \frac{\sqrt{2}\nu_n}{3}, \quad \text{and} \quad \gamma = \frac{3}{4\sqrt{2}}. \tag{9}$$

In Eq. (7), the term $\propto\Omega^2$ arises due to the presence of external magnetic field (which is responsible for Coriolis and Lorentz forces on dust particles), whereas, the term $\propto\gamma$ arises due to the anisotropy (2D geometry). In the absence of rotation ($\Omega = 0$), we recover the 2D KdV equation with a linear damping term (damped 2D KdV equation), where the damping arises due to the neutral drag.

On the other hand, in the absence of collisions ($\nu = 0$), we recover the rotation modified 2D KdV equation [57] for quasilongitudinal nonlinear DLW. Then, in the absence of anisotropic effect (γ does not arise), i.e., in the 1D limit, we obtain the following equation:

$$\frac{\partial}{\partial\xi}\left[\frac{\partial u}{\partial\tau} - \alpha u\frac{\partial u}{\partial\xi} + \beta\frac{\partial^3 u}{\partial\xi^3}\right] = \frac{\Omega^2 u}{\sqrt{2}}.$$

In the literature, this is known as the Ostrovsky's equation [58], which describes the nonlinear internal waves in a rotating ocean.

However, in the absence of both rotation and collision ($\Omega = 0, \nu = 0$), we recover the usual 2D KdV equation (or Kadomstev-Petviashvili equation) [59]. Then, in the 1D limit, the nonlinear dynamics of the longitudinal DLW is governed by the celebrated KdV equation [60]. In the subsequent sections, we investigate the analytical as well as numerical solution of the novel Eq. (7).

III. ANALYTICAL SOLUTION: DECAY OF SOLITONS WITH OSCILLATING TAILS

In this section, we shall investigate analytically the effects of external magnetic field (Coriolis and/or Lorentz force) and dust-neutral collision on localized solutions of the nonlinear dust-lattice waves in 2D crystal. First, we transform Eq. (7) into the following form:

$$\frac{\partial}{\partial\chi}\left[\frac{\partial u}{\partial\tau} - \frac{\alpha k_\xi}{2}\frac{\partial u^2}{\partial\chi} + \beta k_\xi^3\frac{\partial^3 u}{\partial\chi^3} + \frac{\gamma k_\eta^2}{k_\xi}\frac{\partial u}{\partial\chi} + \nu u\right] = \frac{\Omega^2 u}{k_\xi\sqrt{2}}, \tag{10}$$

where $\chi = k_\xi\xi + k_\eta\eta$, k_ξ and k_η are the wave numbers such that $k_\eta = k_\xi \tan\theta$, and θ is the angle that the wave makes with the x axis.

A. Perturbative approach: Decay of solitons

The 2D KdV Eq. (7) or Eq. (10) with $\Omega = 0$ and $\nu = 0$ represents a completely integrable Hamiltonian system that has an infinite set of conservation laws (as in the case of 1D KdV equation, having similar universality) [61]. Let us consider the energy conservation law: Multiplying Eq. (10) (with $\Omega = 0$ and $\nu = 0$) by $u(\chi,\tau)$ and then integrating the resulting equation with respect to χ within the interval $(-\infty,\infty)$ subject to the localized boundary conditions $u(\chi,\tau), \partial_\chi u(\chi,\tau)$ and $\partial_\chi^2 u(\chi,\tau)$ (∂_χ partial derivative with respect to χ) all $\to 0$ as $|\chi| \to \infty$, the following energy equation is obtained:

$$\frac{\partial\mathcal{E}}{\partial\tau} = 0, \quad \mathcal{E} = \frac{1}{2}\int_{-\infty}^{\infty} u^2(\chi,\tau)d\chi, \tag{11}$$

where $\mathcal{E}$ is the soliton energy. This shows that, in the absence of rotation ($\Omega = 0$) and collision ($\nu = 0$), the soliton energy $\mathcal{E}$ is conserved and thus possesses the planar single soliton solution,

$$u(\xi,\eta,\tau) = -N\,\mathrm{sech}^2\sqrt{N}\,\phi, \tag{12}$$

where $\phi = \chi - N\omega\tau$, N is the maximum amplitude of the soliton, ω is the frequency, $U = N\omega$ is the soliton velocity, and the width of the soliton is proportional to $(1/\sqrt{N})$. The parameters N and ω are related by the relation

$$U_f = U - \gamma\frac{k_\eta^2}{k_\xi} = 4N\beta k_\xi^3, \tag{13}$$

with $k_\xi^2 = \alpha/4\beta$. The solution Eq. (12) clearly shows that, for the existence of soliton (localized) solution, $N > 0$ as both $\alpha > 0$ and $\beta > 0$. Thus, the relation Eq. (13) gives us a restriction that for the existence of localized solution, we must have $U_f > 0$.

In the presence of Ω and ν, Eq. (7) [Eq. (10)] does not possess a completely integrable Hamiltonian. In other words, energy of the system is not conserved. To obtain the energy equation, first Eq. (10) is integrated once with respect to χ, which gives

$$\frac{\partial u}{\partial\tau} - \frac{\alpha k_\xi}{2}\frac{\partial u^2}{\partial\chi} + \beta k_\xi^3\frac{\partial^3 u}{\partial\chi^3} + \frac{\gamma k_\eta^2}{k_\xi}\frac{\partial u}{\partial\chi} + \nu u = \frac{\Omega^2}{k_\xi\sqrt{2}}\left[\int_{-\infty}^{\chi} u\,d\chi - \int_{-\infty}^{\infty} u\,d\chi\right], \tag{14}$$

where the second term in the right-hand side appears as the integration constant, which is determined from the boundary conditions $u, du/d\chi \to 0$ as $\chi \to \pm\infty$. Then we apply the energy conservation law, which yields

$$\frac{\partial\mathcal{E}}{\partial\tau} = -2\nu\mathcal{E} + \frac{\Omega^2}{k_\xi\sqrt{2}}\left[\int_{-\infty}^{\infty}\left(u\int_{-\infty}^{\chi} u\,d\acute{\chi}\right)d\chi - \left(\int_{-\infty}^{\infty} u\,d\chi\right)^2\right]. \tag{15}$$

This indicates that the gyration modified 2D damped KdV Eq. (7) [Eq. (9)] is not exactly analytically solvable. However, in the presence of rotation and collision, we can obtain an approximate analytical solution by the soliton perturbation analysis [62,63]. Here, we adopt this perturbation procedure to find an approximate time evolution solution of Eq. (9) with $\Omega \ll 1$ and $\nu \ll 1$ as the perturbed parameters. To apply this perturbation, we assume a slow time-dependent form of the soliton parameter $N = N(\tau)$. In the perturbation analysis [62,63], the leading order one-soliton solution of Eq. (9) can be written as

$$u(\chi,\tau) = -N(\tau)\,\mathrm{sech}^2\sqrt{N(\tau)}\,\phi(\tau), \tag{16}$$

where $\phi(\tau) = \chi - U(\tau)\tau$. To explain the effects of disturbance (here, rotation and dust-neutral collision) on the initial soliton (leading order), the judicial choice is the use of conservation laws [64]. Accordingly [25,62,63], we apply the energy conservation Eq. (15). Finally, substitution of Eq. (16) in Eq. (15), yields the following expressions for soliton energy:

$$\mathcal{E} = \mathcal{E}(0)\exp(-2\nu\tau)\left\{1 + \frac{3\Omega^2}{2\sqrt{2N(0)}\,\nu k_\xi}\left[1 - \exp\left(\frac{2}{3}\nu\tau\right)\right]\right\}^3 \tag{17}$$

and amplitude

$$N(\tau) = N(0)\exp\left(-\frac{4}{3}\nu\tau\right)\left\{1 + \frac{3\Omega^2}{2\sqrt{2N(0)}\,\nu k_\xi}\left[1 - \exp\left(\frac{2}{3}\nu\tau\right)\right]\right\}^2, \tag{18}$$

where $\mathcal{E}(0)$ and $N(0)$ are the initial soliton energy and amplitude.

Let us define a quantity

$$\mathcal{D} = \text{soliton amplitude} \times \text{soliton width}^2,$$

which determines one of the characteristics of a soliton. The above perturbation analysis shows that in the presence of both rotation and dust-neutral collision, $\mathcal{D}$ remains constant as soliton propagates.

In the limit of vanishing magnetic field effect, i.e., rotational effect ($\Omega \to 0$), we recover the usual exponential decay of soliton energy and amplitude due to the dust-neutral collision (neutral drag force) [19,20]:

$$\mathcal{E} = \mathcal{E}(0)\exp(-2\nu\tau) \quad \text{and} \quad N(\tau) = N(0)\exp\left(-\tfrac{4}{3}\nu\tau\right). \tag{19}$$

These solutions clearly show that the dust-neutral collision effect causes the soliton amplitude, soliton energy, and consequently soliton velocity to decay exponentially in time. But, the soliton width increases with time. However, $\mathcal{D}_{\Omega\to 0}$ remains constant and the solitons are weakly dissipative in nature as observed in the experiment of Ref. [19].

In the collisionless limit ($\nu \to 0$), we obtain the following expressions for soliton energy,

$$\mathcal{E} = \mathcal{E}(0)\left[1 - \frac{\Omega^2\tau}{\sqrt{2N(0)}\,k_\xi}\right]^3, \tag{20}$$

and amplitude

$$N(\tau) = N(0)\left[1 - \frac{\Omega^2\tau}{\sqrt{2N(0)}\,k_\xi}\right]^2, \tag{21}$$

under the influence of Lorentz force only. It should be noted that for a soliton solution to exist one must have (soliton width must be real) $N > 0$ and soliton energy $\mathcal{E} > 0$; therefore, the above solutions Eqs. (20) and (21) are physically valid only for $\tau \lesssim \tau_{\rm cr}$. Otherwise, both soliton width and energy become negative and no soliton solution exists. Actually, both the soliton amplitude and energy completely vanish at a finite time:

$$\tau_{\rm cr} = \frac{\sqrt{2N(0)}\,k_\xi}{\Omega^2} = \frac{1}{\Omega^2}\sqrt{\frac{\alpha N(0)}{2\beta}}. \tag{22}$$

However, the value of $\tau_{\rm cr}$ provides a good estimation of a characteristic lifetime of a soliton in a strongly coupled complex (dusty) plasma in presence of weak rotational effect (weak magnetic field). Thus, the solitonic structures exist for $0 \leqslant \tau < \tau_{\rm cr}$.

The above solution Eqs. (20) and (21) reveal that the Coriolis force and or Lorentz force on dust particles causes the soliton amplitude, soliton energy, and consequently soliton velocity to decay algebraically with time, whereas, the soliton width increases with time for $\tau < \tau_{\rm cr}$. But, $\mathcal{D}_{\nu\to 0}$ remains constant as before. In terms of the actual parameter, the critical time is written as

$$t_{\rm cr} = \frac{\sqrt{2}}{\Omega_r}\left(\frac{\rho_{\rm sd}}{\mathcal{W}}\right), \tag{23}$$

where $\rho_{\rm sd}(\propto C_{\rm DL}/\Omega_r)$ is the dust-acoustic gyroradius and $\mathcal{W}\{\propto[2\beta/\alpha N(0)]^{1/2}\}$ is the spatial width of the soliton. Thus, the lifetime of a soliton increases with the decreases of the strength of the external magnetic field.

Note that the above solution Eqs. (17)–(21) are derived from the approximated (leading order) soliton solution, but holds fairly well for dissipative perturbations [62–64]. The higher-order terms in the perturbation analysis introduce only corrections (the change in amplitude, velocity, and width remain the same as obtained in the leading order approximation) [62,63].

B. Oscillating tail formation

In the preceding section, we have derived the analytical solution of Eq. (7) [Eq. (10)] perturbatively with the help of dissipative perturbation technique. However, here, we present an exact analysis of stationary localized solutions of Eq. (7) [Eq. (10)]. Therefore, to investigate the possible localized (soliton-like) solution of Eq. (10), we transform this equation to the stationary frame $\phi = \chi - U\tau$ and obtain the following nonlinear ordinary differential equation:

$$\beta k_\xi^3 \frac{d^4u}{d\phi^4} - \frac{\alpha k_\xi}{2}\frac{d^2u^2}{d\phi^2} - U_f\frac{d^2u}{d\phi^2} + \nu\frac{du}{d\phi} = \frac{\Omega^2 u}{\sqrt{2}k_\xi}. \tag{24}$$

Now we start to analyze this equation by finding decaying asymptotics of its localized solutions in the limit $\phi \to \infty$ ($\chi \to \infty$), as we are interested only in the soliton-like solutions. In this limit, the nonlinear term is negligible so that we can analyze asymptotics of the exponentially decaying solutions of the following linear differential equation:

$$\beta k_\xi^3 \frac{d^4u}{d\phi^4} - U_f\frac{d^2u}{d\phi^2} + \nu\frac{du}{d\phi} = \frac{\Omega^2 u}{\sqrt{2}k_\xi}. \tag{25}$$

The general form of the solutions to Eq. (25) is $u = Ae^{\lambda\phi}$, where λ is the root (eigen value) of the corresponding fourth-order algebraic equation given by

$$\beta k_\xi^3\lambda^4 - U_f\lambda^2 + \nu\lambda - \frac{\Omega^2}{\sqrt{2}k_\xi} = 0. \tag{26}$$

Note that we have already seen that for localized solution $U_f > 0$. Now for decaying solutions, we must have Re $\lambda < 0$. Absence of collision ($\nu = 0$) leaves us the following two possibilities of the decaying solutions:

$$\lambda = -\frac{1}{\sqrt{2\beta k_\xi^3}}\left[U_f \pm \sqrt{U_f^2 + 4\frac{\beta\Omega^2 k_\xi^2}{\sqrt{2}}}\right]^{\frac{1}{2}}. \tag{27}$$

Every localized solution of Eq. (25) must have one of the asymptotics, Eq. (27). The above expression clearly shows that the parameter λ has a purely imaginary value. Thus, the corresponding localized solutions of Eq. (25) must have oscillating tails.

On the other hand, in the absence of rotation ($\Omega = 0$), Eq. (26) reveals that the parameter λ has imaginary part only if

$$\nu^2 > \frac{4}{27}\frac{U_f^3}{\beta k_\xi^3}.$$

However, this inequality is hardly satisfied for the laboratory plasma condition [13,19], where $\nu = O(10^{-1} - 10^{-3})$. Thus, there is no oscillating tail of the localized solutions only for the collision that can be easily seen from our simulation result.

It is important to note that the existence of decaying solution of the linear Eq. (25) is not a sufficient condition for the existence of the corresponding localized (soliton-like) solution of the nonlinear Eq. (10). However, it assures the existence of oscillating tails of the localized solutions (if they exist). In the next section, the numerical simulation of Eq. (10) confirms this tail formation of the soliton, in the presence of rotation (Coriolis force and/or Lorentz force).

IV. NUMERICAL SIMULATION

We are interested to find the solution of Eq.(7) [Eq. (10)] with its full generality. We have already seen that in the presence of rotation ($\Omega \neq 0$) and dust-neutral collision ($\nu \neq 0$), Eq.(7) [Eq. (10)] is not an exactly integrable Hamiltonian system. Therefore, to investigate the effect of (magnetic field) Lorentz force-induced gyration and dust-neutral collisions on solitons in a quasi-two-dimensional crystal, we simulate the nonlinear Eq. (10) numerically with the help of a MATHEMATICA-based finite difference scheme. The numerical simulations are carried out for the following typical laboratory complex plasma parameters: $T_e = 3$ eV, $T_i = 0.03$ eV, $m_i = 6.69 \times 10^{-26}$ kg, $n_i = 3 \times 10^{14}$ m^{-3}, and $B_0 = 1$ T. The dust-particle (melamine formaldehyde) mass density 1.5×10^3 kg m^{-3}, $a = 2.4$ μm (so that $m_d = 8.7 \times 10^{-14}$ kg) and $T_d = 0.03$ eV. These parameters estimate, $\lambda_D \simeq \lambda_{Di} = 75$ μm, $\omega_{pi} = 3.6 \times 10^6$ rad s^{-1}, $\omega_{ci} = 2.4 \times 10^6$ rad s^{-1} (so that $\sqrt{f} = \omega_{pi}/\omega_{ci} = 1.5$), $\rho_i = 111$ μm, and $\rho_e = 4.2$ μm, implying $\beta_{B_i} = 0.02$ and $\beta_{B_e} = 0.6$. This shows that the curvature effect of the ion (electron) will not significantly modify the dust-charging characteristics. Thus, the OML theory for dust-charging yields $Q_{\text{eff}}(= Q) = -5 \times 10^3$ e ($z = 1$) and this yields, $n_d = 5.3 \times 10^{10}$ m^{-3}, $\Delta = 165$ μm, $\kappa = 2.2$, $\omega_L = 10^2$ rad s^{-1}, and $\Gamma = 7273$. The screened coupling parameter $\Gamma^* = 806$, the modified screening parameter $\bar{\kappa} = 1.5$, and the modified coupling parameter $\bar{\Gamma}^* = 721$. Thus, the presence of an external magnetic field reduces the strength of the screened Coulomb potential. However, the estimated values (Γ^* and $\bar{\Gamma}^*$) are large enough to predict a crystalline state in SCCP in the presence of an external magnetic field. The estimated dust-cyclotron frequency $\omega_{\text{cd}} = 0.01$ rad s^{-1}, whereas, the observed [39] rotational frequency $\omega \sim 1$ rad s^{-1} for $B_0 = 1$ T (much larger than the dust-cyclotron frequency). Thus, the rotation is mainly due to the Coriolis force on the dust particles. The angle of propagation is taken as $\theta = 10^\circ$.

In the absence of rotation ($\Omega = 0$) and collision ($\nu = 0$), the 2D KdV Eq. (7) [Eq. (10)] possesses a single-soliton solution. Therefore, for the time-dependent numerical simulation, we use the single-soliton solution as the initial waveform: $u(\chi,0) = -N\ \text{sech}^2\sqrt{N}\ \chi$, $\chi \in [-L,L]$, where L is the spatial length. The boundary conditions are $u(\pm L,\tau) = -N\ \text{sech}^2(\pm\sqrt{N}\ L)$ and $u_\chi(-L,\tau) = 0 = u_\chi(L,\tau)$. To obtain adequate results for the computation, we take $L = 30$ and $N = 1$.

At first we solve the 2D KdV equation [Eq. (10), with $\Omega = 0$ and $\nu = 0$], which is shown in Fig. 2 [left figure]. This is the usual single-soliton solution. Then we introduce the

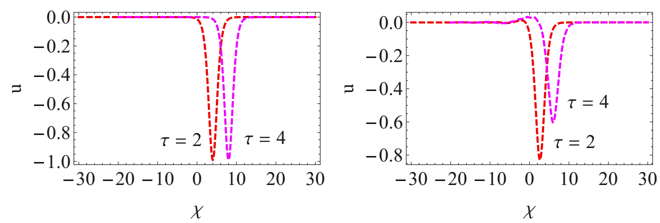

FIG. 2. (Color online) Time evaluation of quasilongitudinal solitons in 2D complex plasma. The numerical solution of Eq. (10). The left figure is drawn for $\nu = 0$ and $\Omega = 0$, which is the usual dust lattice soliton. The right figure is drawn for $\Omega = 0$ and $\nu = 0.1$. The curves in this figure show the neutral drag force induced weakly dissipative quasilongitudinal solitons in 2D complex plasma.

dust-neutral collisional effect with $\nu = 0.1$ in our numerical simulation. The results are shown in Fig. 2 [right figure]. These figures show that the amplitude of the soliton (width of the soliton) decreases (increases) with time due to the dust-neutral collision. The comparative study between the curves in the left and right figures demonstrate that the soliton velocity also decreases in the presence of collision. Actually, these figures show the weakly dissipative nature of the quasilongitudinal solitons in 2D dusty plasma crystal as observed in the experiment [19]. However, no soliton tail formation is observed, which is consistent with the analytical result of the previous section.

Next, we investigate the effect of rotation in the formation of soliton. We take $\nu = 0$ and $\Omega = 0.1$ in the numerical simulation and the results are plotted in Fig. 3. The curves in these figures show that the soliton amplitude decreases and the spatial width widens accordingly due to the effect of rotation and, finally, oscillating tails are formed. Thus, the time-dependent numerical simulation exhibits the same nature of the decaying soliton with oscillating tails as predicted by the analytical analysis.

Finally, we solve Eq. (10) with its full generality. The simulation parameters are $\Omega = 0.1$ and $\nu = 1$. The simulation results are shown in Fig. 4. The curves in these figures show qualitatively the same nature as in Fig. 3. The only difference is quantitative. In this case the amplitude of the solitons and also tails become more damped in the presence of dust-neutral collision.

The above discussions clearly demonstrate that the results obtained by the numerical simulation of Eq. (10) with

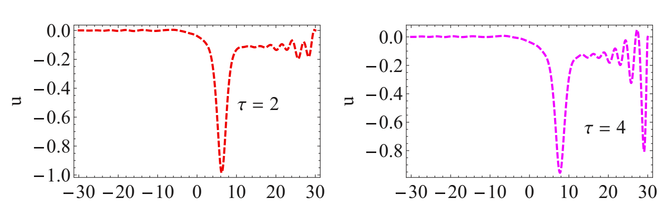

FIG. 3. (Color online) Time evaluation of quasilongitudinal solitons in 2D complex plasma in the presence of rotation only. The numerical solution of Eq. (10) with $\Omega = 0.1$ and $\nu = 0$. These figures clearly demonstrate the formation of oscillating tails of solitons due to rotation and also the algebraic decay of the amplitude.

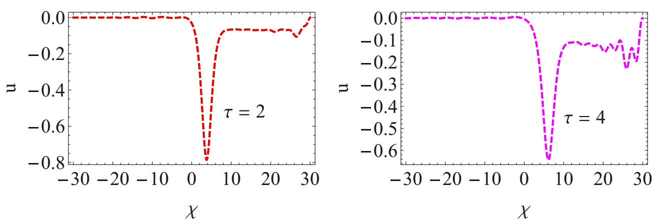

FIG. 4. (Color online) Time evaluation of quasilongitudinal solitons in 2D complex plasma in the presence of both rotation and dust-neutral collisions. The numerical solution of Eq. (10) with $\Omega = 0.1$ and $\nu = 1$.

plasma parameters relevant to SCCP experiment are in good agreement with the analytical results derived in the previous section.

V. DISCUSSIONS

In this paper, we investigate the effects of neutral drag force due to dust-neutral collision and Coriolis force and/or Lorentz force due to the external magnetic field on the formation of quasilongitudinal solitons in 2D strongly correlated dusty plasma. The dynamics of the quasilongitudinal nonlinear wave is governed by a novel equation, namely, a gyration modified damped 2D KdV equation. The equation is analyzed analytically with the help of the dissipative perturbation technique. This equation is also numerically simulated with the typical experimental plasma parameters. The numerical results agree well with the analytical results. Both results reveal that the solitons are compressive in nature. This can easily be seen from the fact that the velocity of the particles moving in the wave is given by

$$U_x = \frac{\partial d_l}{\partial t} = -\epsilon C_{\mathrm{DL}} M u > 0,$$

as the Mach number $M = U/C_{\mathrm{DL}} > 0$ and $u < 0$. Thus, the particles move forward in the direction of the soliton propagation. As a consequence, the dust number density perturbation n_d (normalized in units of equilibrium dust density n_{d0}), given by [65]

$$n_d \simeq -u \, (\Rightarrow U_x \simeq \epsilon C_{\mathrm{DL}} M n_d > 0)\,,$$

corresponds to the increase in the dust-particle number density as the soliton propagates. This is in agreement with the experimental observations [13,15,16]. Also, the derived quasilongitudinal compressional solitons are always stable against longitudinal perturbations as solitons are supersonic $M > 1$. However, the stability conditions against transverse perturbations [59], not studied here, have to be studied separately.

In the absence of external magnetic field, Eq. (7) reduces to the damped 2D KdV equation that governs the dynamics of the weakly nonlinear quasilongitudinal DLW. The analytical and numerical results [Eq. (19) and Fig. 2] demonstrate that, in this case, due to the neutral drag force, the soliton energy, amplitude, and velocity decays exponentially with time, whereas, the spatial width of the soliton increases with time accordingly. However, the parameter $\mathcal{D}_{\Omega\to 0}$ remains constant throughout the motion. In the experiment in Ref. [19], it was found that the soliton parameters (amplitude and velocity) decrease with time, whereas, width of the soliton increases accordingly and $\mathcal{D}_{\Omega\to 0}$ approximately remains constant as the soliton propagates. Thus, the results of the present investigation are in qualitative agreement with the experimental observations [19]. Moreover, recently, dissipative dark solitons are observed in a three-dimensional strongly coupled complex plasma [23]. This experimental observation also confirms the dissipation of solitons in complex plasma due to the neutral drag.

In the absence of neutral drag force, Eq. (7) reduces to the rotation-modified 2D KdV equation for the dynamics of the weakly nonlinear quasilongitudinal DLW. Contrary to the dynamics of the soliton in the presence of collision, in this case the soliton amplitude, energy, and velocity decays algebraically with time $\tau < \tau_{\mathrm{cr}}$ and width increases accordingly [Eqs. (20) and (21)] so that the quantity $\mathcal{D}_{\nu\to 0}$ is constant. This critical time $\tau_{\mathrm{cr}} \propto \Omega^{-2} = (\omega_L/\Omega_r)^2$ [Eq. (22)] determines the lifetime of a soliton in a dusty plasma crystal in the presence of Coriolis force and/or Lorentz force. The lifetime of a soliton decreases (increases) with the increase (decrease) of the strength of the external magnetic field. The analytical result and numerical simulation also predict the oscillating tail formation of the quasilongitudinal solitons in a 2D strongly coupled complex plasma due to the rotation [Eq. (27) and Figs. 3 and 4]. In connection with the complex plasma experiment, we must mention that we have not encountered any experimental observations of the quasilongitudinal solitons in 2D strongly coupled complex plasma in the presence of a magnetic field. It would be very interesting to look at this situation in a laboratory. We hope that in the future, such a type of dissipative quasilongitudinal soliton in the presence of an external magnetic field could be observed in SCCP experiments.

ACKNOWLEDGMENT

The author thanks the referees for the careful reading and offering constructive suggestions to improve the manuscript.

[1] V. E. Fortov, A. V. Ivlev, S. A. Khrapak, A. G. Khrapak, and G. E. Morfill, Phys. Rep. **421**, 1 (2005).

[2] G. E. Morfill and A. V. Ivlev, Rev. Mod. Phys. **81**, 1353 (2009).

[3] S. Hamaguchi, R. T. Farouki, and D. H. E. Dubin, Phys. Rev. E **56**, 4671 (1997).

[4] J. H. Chu and L. I, Phys. Rev. Lett. **72**, 4009 (1994).

[5] H. M. Thomas, G. E. Morfill, V. Demmel, J. Goree, B. Feuerbacher, and D. Möhlmann, Phys. Rev. Lett. **73**, 652 (1994).

[6] H. M. Thomas and G. E. Morfill, Nature (London) **379**, 806 (1996).

[7] M. Chaudhuri, A. V. Ivlev, S. A. Khrapak, H. M. Thomos, and G. E. Morfill, Soft. Matter **7**, 1287 (2011).

[8] S. Nunomura, D. Samsonov, and J. Goree, Phys. Rev. Lett. **84**, 5141 (2000).
[9] S. Nunomura, J. Goree, S. Hu, X. Wang, and A. Bhattacharjee, Phys. Rev. E **65**, 066402 (2002).
[10] S. Nunomura, J. Goree, S. Hu, X. Wang, A. Bhattacharjee, and K. Avinash, Phys. Rev. Lett. **89**, 035001 (2002).
[11] P. K. Kaw and A. Sen, Phys. Plasmas **5**, 3552 (1998).
[12] J. Pramanik, G. Prasad, A. Sen, and P. K. Kaw, Phys. Rev. Lett. **88**, 175001 (2002).
[13] D. Samsonov, J. Goree, Z. W. Ma, A. Bhattacharjee, H. M. Thomas, and G. E. Morfill, Phys. Rev. Lett. **83**, 3649 (1999).
[14] D. H. E. Dubin, Phys. Plasmas **7**, 3895 (2000).
[15] D. Samsonov, J. Goree, H. M. Thomas, and G. E. Morfill, Phys. Rev. E **61**, 5557 (2000).
[16] A. Melzer, S. Nunomura, D. Samsonov, Z. W. Ma, and J. Goree, Phys. Rev. E **62**, 4162 (2000).
[17] F. Melandso, Phys. Plasmas **3**, 3890 (1996).
[18] S. V. Vladimirov, P. V. Shevchenko, and N. F. Cramer, Phys. Rev. E **56**, R74 (1997).
[19] D. Samsonov, A. V. Ivlev, R. A. Quinn, G. Morfill, and S. Zhdanov, Phys. Rev. Lett. **88**, 095004 (2002).
[20] S. K. Zhdanov, D. Samsonov, and G. E. Morfill, Phys. Rev. E **66**, 026411 (2002).
[21] S. Nunomura, S. Zhdanov, G. E. Morfill, and J. Goree, Phys. Rev. E **68**, 026407 (2003).
[22] B. Farokhi, I. Kourakis, and P. K. Shukla, Phys. Plasmas **13**, 122304 (2006); W. Duan, J. Parkes, and M. Lin, *ibid.* **12**, 022106 (2005).
[23] R. Heidemann, S. Zhdanov, R. Sütterlin, H. M. Thomas, and G. E. Morfill, Phys. Rev. Lett. **102**, 135002 (2009).
[24] P. Bandyopadhyay, G. Prasad, A. Sen, and P. K. Kaw, Phys. Rev. Lett. **101**, 065006 (2008).
[25] S. Ghosh, M. R. Gupta, N. Chakrabarti, and M. Chaudhuri, Phys. Rev. E **83**, 066406 (2011).
[26] S. K. Sharma, A. Boruah, and H. Bailung, Phys. Rev. E **89**, 013110 (2014).
[27] D. Samsonov, S. K. Zhdanov, R. A. Quinn, S. I. Popel, and G. E. Morfill, Phys. Rev. Lett. **92**, 255004 (2004).
[28] S. Ghosh, JETP Lett. **87**, 281 (2008); **88**, 702 (2008); Contrib. Plasma Phys. **48**, 569 (2008).
[29] S. Ghosh, Phys. Plasmas **16**, 103701 (2009).
[30] S. V. Vladimirov, G. E. Morfill, V. V. Yaroshenko, and N. F. Cramer, Phys. Plasmas **10**, 2659 (2003).
[31] G. Uchida, U. Konopka, and G. Morfill, Phys. Rev. Lett. **93**, 155002 (2004).
[32] K. Jiang, Y. Song, and Y. Wang, Phys. Plasmas **14**, 103708 (2007); B. Farokhi, M. Shahmansouri, and P. K. Shukla, *ibid.* **16**, 063703 (2009).
[33] M. Schwabe, U. Konopka, P. Bandyopadhyay, and G. E. Morfill, Phys. Rev. Lett. **106**, 215004 (2011).
[34] E. Thomas, Jr., R. L. Merlino, and M. Rosenberg, Plasma Phys. Controlled Fusion **54**, 124034 (2012); E. Thomas Jr., R. L. Merlino, and M. Rosenberg, IEEE Trans. Plasma Sci. **41**, 811 (2013).
[35] H. Kählert, J. Carstensen, M. Bonitz, H. Löwen, F. Greiner, and A. Piel, Phys. Rev. Lett. **109**, 155003 (2012).
[36] M. Bonitz, H. Kählert, T. Ott, and H. Löwen, Plasma Sources Sci. Technol. **22**, 015007 (2013).
[37] U. Konopka, D. Samsonov, A. V. Ivlev, J. Goree, V. Stenberg, and G. E. Morfill, Phys. Rev. E **61**, 1890 (2000).
[38] N. Sato, Bull. Am. Phys. Soc. **45**, 157 (2000).
[39] N. Sato, G. Uchida, Y. Kaneko, S. Dhimizu, and S. Lizuka, Phys. Plasmas **8**, 1786 (2001).
[40] P. K. Kaw, K. Nishikawa, and N. Sato, Phys. Plasmas **9**, 387 (2002).
[41] F. M. H. Cheung, N. J. Prior, L. W. Mitchel, A. A. Samarian, and B. W. James, IEEE Trans. Plasma Sci. **31**, 112 (2003).
[42] L. Hou, Y. Wang, and Z. L. Mišković, Phys. Plasmas **12**, 042104 (2005).
[43] O. Ishihara and N. Sato, IEEE Trans. Plasma Sci. **29**, 179 (2001).
[44] O.Ishihara, T. Kamimura, K. I. Hirose, and N. Sato, Phys. Rev. E **66**, 046406 (2002).
[45] V. N. Tsytovich, N. Sato, and G. E. Morfill, New J. Phys. **5**, 43 (2003).
[46] V. N. Tsytovich and S. V. Vladimirov, IEEE Trans. Plasma Sci. **32**, 659 (2004).
[47] J. E. Allen, Phys. Scr. **45**, 497 (1992).
[48] M. Lampe, G. Joyce, G. Ganguli, and V. Gavrishehaka, Phys. Plasmas **7**, 3851 (2000).
[49] Y. Tomita, G. Kawamura, T. Yamada, and O. Ishihara, J. Plasma Fusion Res. SERIES **8**, 273 (2009).
[50] M. Chaudhuri, S. Khrapak, R. Kompaneets, and G. E. Morfill, IEEE Trans. Plasma Sci. **38**, 818 (2010).
[51] M. Nambu, M. Salimullah, and R. Bingham, Phys. Rev. E **63**, 056403 (2001).
[52] P. K. Shukla and J. T. Mendonça, Phys. Scr. T **113**, 82 (2004).
[53] K. Avinash, P. K. Shukla, and R. L. Merlino, Phys. Scr. **86**, 035504 (2012).
[54] V. V. Yaroshenko, G. E. Morfill, D. Samsonov, and S. V. Vladimirov, New J. Phys. **5**, 18 (2003).
[55] V. V. Yaroshenko, G. E. Morfill, D. Samsonov, and S. V. Vladimirov, IEEE Trans. Plasma Sci. **32**, 675 (2004).
[56] T. Tanuiti, Suppl. Prog. Theor. Phys. **55**, 1 (1974).
[57] S. Ghosh and M. R. Gupta, Phys. Plasmas **17**, 034505 (2010).
[58] L. A. Ostrovsky, Oceanology **18**, 119 (1978).
[59] B. B. Kadomstev and V. I. Petviashvili, Sov. Phys. Dokl. **15**, 539 (1970).
[60] D. Korteweg and G. de Vries, Philos. Mag. **39**, 422 (1895).
[61] V. Yu. Belashov and S. V. Vladimirov, *Solitary Waves in Dispersive Complex Media* (Springer-Verlag, Berlin/Heidelberg, 2005), p. 140.
[62] V. I. Karpman and E. M. Maslov, Sov. Phys. JETP **46**(2), 281 (1977).
[63] R. L. Herman, J. Phys. A **23**, 4719 (1990).
[64] A. C. Newell, *Solitons in Mathematics and Physics* (SIAM, Philadelphia, PA, 1985).
[65] P. K. Shukla, Phys. Lett. A **300**, 282 (2002).